Zhou *et al.*
Chinese Journal of Mechanical Engineering (2022) 35:111
https://doi.org/10.1186/s10033-022-00787-0

Chinese Journal of Mechanical Engineering

ORIGINAL ARTICLE

Open Access

Variational Wavelet Ensemble Empirical (VWEE) Denoising Method for Electromagnetic Ultrasonic Signal in High-Temperature Environment with Low-Voltage Excitation

Jinjie Zhou[1*], Shuaijie Zhao[1], Yang Zheng[2], Xingquan Shen[1] and Jitang Zhang[1]

Abstract

Low excitation voltage for an electromagnetic acoustic transducer (EMAT) is necessary for the petrochemical equipment and facilities inspection, which work at high-temperatures, to avoid potential explosion. However, low excitation voltage causes low signal-to-noise ratio (SNR) signals that are difficult to extract features, especially in a high-temperature environment, which causes high noise. In this study, a denoising method called the variational wavelet ensemble empirical (VWEE) method was proposed by combining the advantages of the variational modal decomposition (VMD), wavelet threshold (WT) denoising, and ensemble empirical mode decomposition (EEMD) methods. To validate the VWEE method, EMAT signals obtained in the temperature range of 25 to 700 °C were analyzed. The results show that, compared with VMD, WT and empirical mode decomposition denoising methods, the SNR of proposed method is improved more than two times. The VWEE method dramatically improved the SNR of a high-temperature EMAT signal and enhanced the accuracy of defect echos extraction.

Keywords: EMAT, High temperature, Low excitation voltage, SNR

1 Introduction

Nondestructive testing technology is widely used in industry [1–3]. Corrosion caused by the environment and flowing media gradually reduces the thickness and weakens the strength of pressure pipeline and container, which eventually leads to a catastrophic accident [4]. Online monitoring of the wall thickness and internal damage using an electromagnetic acoustic transducer (EMAT) [5–7] is an effective way to avoid the above incidents. In practice, high-voltage excitation is often used to improve the echo energy. However, for pipeline and container with flammable and explosive media, which usually works at high temperature and pressure, such as boiler or reactor, the excitation voltage should be low for safety. The low-voltage excitation results in a low signal-to-noise ratio (SNR) and buries the valuable information in noise, which causes the failure of the wall thickness and the defect detection [8–10]. To solve the above problem, a new denoising method or theory is needed to effectively extract useful information in this high noise environment.

Given the low SNR in acoustic detection, many studies have been conducted to improve the useful signal quality. Kubinyi et al. [11, 12] proposed a stationary wavelet packet denoising method and proved that the SNR of EMAT signals was two time higher than that of the split-spectrum processing or standard wavelet filtering

*Correspondence: zhoujinjiechina@126.com

[1] School of Mechanical Engineering, North University of China, Taiyuan 030051, China
Full list of author information is available at the end of the article

algorithm through experiments. They also created a signal filtering method based on information fusion, and the method had a better effect on the studied acoustic signals compared with the digital filtering or wavelet denoising method. Lei et al. [13] proposed an improved singular value decomposition (SVD) denoising method based on a fitted threshold and adopted the piecewise regression model to find the appropriate threshold, which had a good denoising effect on the EMAT signals. Legendre et al. [14] proposed a wavelet-based approach to enhance the acoustic signals received during composite material detection. Huang et al. [15] proposed an algorithm using envelope regulation technology and applied it to EMAT surface wave experimental data. The experimental results showed that the advanced algorithm could significantly reduce the overall noise level of the signal, suppress the random fluctuation of the signal waveform, and maintain the main characteristics of the signal.

Different types of wavelet basis functions and decomposition layers have a large influence on denoising when a wavelet transform was used in signal processing. Huang et al. [16] proposed empirical mode decomposition (EMD) as an adaptive signal processing method. The signal was decomposed into a series of intrinsic mode function (IMF) components representing signal characteristics from high to low frequency. Sun et al. [17] proposed a method based on modified EMD to denoise signals with horn-type noise, which improved the SNR of the acoustic echo signals. However, the computational cost was too high. Wu and Huang [18] proposed ensemble empirical mode decomposition (EEMD), which selected the set with a white noise signal and took the mean value as the final result. Yu et al. [19] proposed an EEMD method to extract the characteristics of acoustic echo signals. The method reduced the modal mixture generated by the EMD to a certain extent. Dragomiretskiy et al. [20] proposed a variable scale non-stationary signal analysis method, variational mode decomposition (VMD), which could decompose complex signals into the form of a multiple single-component AM-FM signal sum. The number of modes in the decomposition process could be determined adaptively. Huang et al. [21] proposed an improved shear horizontal guided wave pattern recognition method based on the VMD algorithm and time-of-flight extraction method based on the synchronous compression wavelet transform algorithm, which helped to improve the sensitivity and accuracy of shear horizontal wave defect detection. Si et al. [22] proposed an improved VMD fusion wavelet method to suppress the high-frequency narrowband noise and normal noise in EMAT signals with a large lift-off detection condition. Wei et al. [23] proposed an improved empirical variational mode decomposition (EVMD) method for acoustic echo signal processing that could effectively identify the coal-rock interface. So far, VMD algorithm has been widely applied in various fields [24–27]. For the reviewed denoising methods above, the filtering effect can easily produce waveform distortion in EMD. The IMF decomposed by the EEMD is affected by noise and cannot express the real physical meaning when the signal noise is severe. The VMD algorithm requires the value of K to be set beforehand, and the smaller or larger value of K will result in the modal component information losting or over-decomposition.

Based on the above shortcomings, this study proposes a new denoising method called variational wavelet ensemble empirical (VWEE) denoising. The theory and principle of this method are first introduced. An experimental system was developed to acquire signals at different excitation voltages and temperatures. Lastly, the comparison among the VMD, wavelet threshold (WT), EMD, and VWEE denoising methods for the measured signal for different excitation voltage and temperatures were given to verify the feasibility and effectiveness of the proposed method.

2 Basic Theory

2.1 Principle of EMAT Detection

Figure 1 shows the structure of an EMAT, which consists of three parts: a coil, a magnetic field provided by a permanent magnet, and a tested sample which should be conductive or magnetic.

The magnet creates a magnetic field B_S that acts on the coil. Then the excitation current density J_c is conducted in the coil and induces a vortex J_e on the surface of the sample. The moving eddies in the vortex produce Lorentz forces in the magnetic fields B_S. When the tested sample is ferromagnetic, with the joint action of the Lorentz force $f^{(L)}$, magnetostrictive force $f^{(fms)}$, and

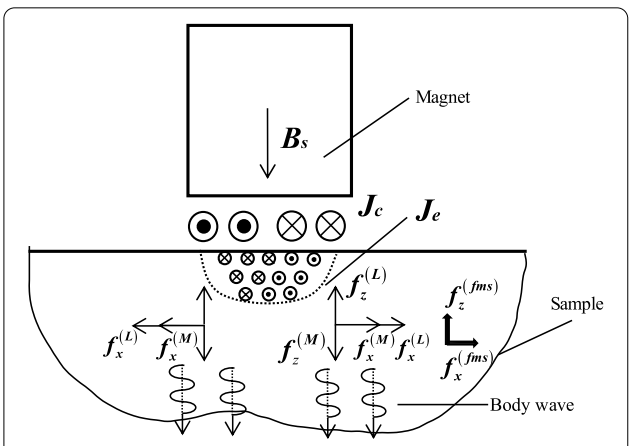

Figure 1 Basic principles and components of EMAT

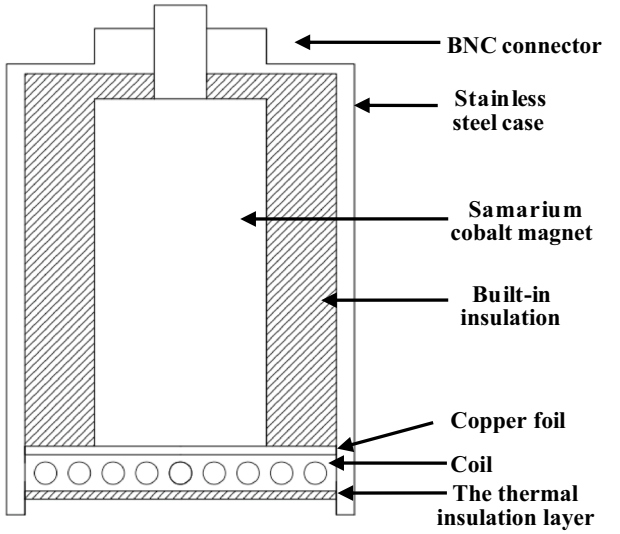

Figure 2 Structure of high-temperature EMAT

magnetization force $f^{(M)}$, a mass point within the skin depth of the specimen surface will vibrate and form acoustic waves [28]. The acoustic reception is based on the reverse process.

2.2 Development of High-temperature EMAT

As shown in Figure 2, the high-temperature EMAT mainly included a high-temperature-resistant bayonet nut connector (BNC) joint, stainless steel house, samarium cobalt magnet, built-in heat insulation layer, copper foil, coil, and heat insulation layer. First, samarium cobalt magnets were used as permanent magnets, which had a high Curie point and could be used for a long time at high-temperatures environment. Second, the coil adopted a spiral coil structure. The inner diameter of the coil was 2.25 mm. The outer diameter was 18.25 mm. The coil was wound 25 times. The wire diameter was 0.12 mm, and the magnet and the coil were separated by 2 mm thick copper foil, which was conducive to electromagnetic shielding. To eliminate any effect of the heated sample on the coil, the coil was raised 2 mm and protected in a ceramic sleeve. Finally, the structure design of the double insulation layer effectively reduced the influence of the heat source on the internal coil and the permanent magnet, ensuring that the EMAT could work at a high temperature for a long time. The highest temperature detected by a high-temperature EMAT was up to 800 °C through testing, ensuring the effectiveness of the experimental data.

3 VWEE Denoising Method

In an EMAT measurement experiment, the echo carries useful information. Because the echo is an unsteady signal, the traditional Fourier transform and other methods cannot be used. In this method, the signal detected by the high-temperature EMAT is decomposed using VMD first to filter out the low- and high-frequency noise signals. Then, WT is used to enhance the denoising effect and filter out the same frequency noise. Finally, the denoising signal is decomposed by EEMD to extract the echo signal.

3.1 Filter Low- and High-frequency Signals

In the time and frequency domain diagrams, echo signals and some high-frequency electrical noise can be found from the EMAT signals. Since the transmitting signal frequency is set in advance, the effective echo signal center frequency is distributed near the transmitting frequency. By analyzing the theory and principle of the existing denoising methods, the VMD method can be used to separate the signal in the frequency domain.

VMD is a non-recursive signal processing method that is different from obtaining components recursively with the traditional EMD algorithm [20], which can be used to separate low- and high-frequency signals. By constructing a constrained variational model, the modal estimation is transformed into a variational problem. The signal is decomposed into a series of modal components around the central frequency with good sparsity among each modal component.

The VMD method decomposes a signal f into a mode function u_k with K orders center frequency ω_k according to the preset scale parameter K. Then the variational constraint problem can be obtained with the following equation [20]:

$$\begin{cases} \min\limits_{\{u_k\},\{\omega_k\}} \left(\sum\limits_{k=1}^{K} \left\| \partial_t \left[\left(\delta(t) + \frac{j}{\pi t} \right) \times u_k(t) \right] e^{-j\omega_k t} \right\|_2^2 \right), \\ \sum\limits_{k=1}^{K} u_k = f, \end{cases} \tag{1}$$

where ∂_t is the partial derivative of the function at time t and $\delta(t)$ is the unit impulse function.

By introducing the augmented Lagrange function L, the constrained problem is transformed into an unconstrained problem:

$$L(\{u_k\},\{\omega_k\},\lambda) = \alpha\sum_{k=1}^{K}\left\|\partial_t\left[\left(\delta(t)+\frac{j}{\pi t}\right)\times u_k(t)\right]e^{-j\omega_k t}\right\|_2^2 + \left\|f(t)-\sum_{k=1}^{K}u_k(t)\right\|_2^2 + \left\langle\lambda(t),f(t)-\sum_{k=1}^{K}u_k(t)\right\rangle, \tag{2}$$

where α is the penalty factor that is used to ensure the signal reconstruction accuracy in the presence of Gaussian noise, λ is the Lagrange multiplier, and <> denotes the inner product of the vectors.

The above variational problem was solved with the alternate direction multiplier algorithm, and the saddle point of the above augmented Lagrange function was obtained by alternately updating u_k^{n+1}, ω_k^{n+1}, and λ_k^{n+1}, which are the optimal solutions of Eq. (2). In the expression, u_k^{n+1} is the modal function at the n+1 cycle, ω_k^{n+1} is the center frequency of the power spectrum of the current modal function, and λ_k^{n+1} is the multiplication operator at the n+1 cycle.

Then, the modal component u_k and the central frequency ω_k that are obtained by

$$\hat{u}_k^{n+1}(\omega) = \frac{\hat{f}(\omega)-\sum_{i\neq k}\hat{u}_i(\omega)+\frac{\hat{\lambda}(\omega)}{2}}{1+2\alpha(\omega-\omega_k)^2}, \tag{3}$$

$$\omega_k^{n+1} = \frac{\int_0^\infty \omega\left|\hat{u}_k(\omega)\right|^2 d\omega}{\int_0^\infty \left|\hat{u}_k(\omega)\right|^2 d\omega}, \tag{4}$$

where $\hat{u}_k^{n+1}$, $\hat{f}$ and $\hat{\lambda}_k^{n+1}$ represent the corresponding Fourier transforms of u_k^{n+1}, f and λ_k^{n+1}, respectively, and α is the penalty factor.

For a given decision accuracy e>0, when Eq. (5) is satisfied, the decomposition iteration stops, and the final modal component $\widehat{u}_k$ and the corresponding central frequency $\widehat{u}_k$ are obtained by

$$\sum_{k=1}^{k}\left(\left\|\hat{u}_k^{n+1}-\hat{u}_k^n\right\|_2^2 \Big/ \left\|\hat{u}_k^n\right\|_2^2\right) < e. \tag{5}$$

With VMD, the choice of parameters was very important. The traditional VMD algorithm required the value K to be set in advance, which meant that the signal was decomposed into K modes. When K=4, the spectrum corresponding to the eigenmode component was as shown in Figure 3, which could better distinguish the noise signals with different frequencies. As shown in Figure 3, the IMF2 was around the excitation frequency. The VMD algorithm could decompose the signal into independent modes and estimate the center frequency of

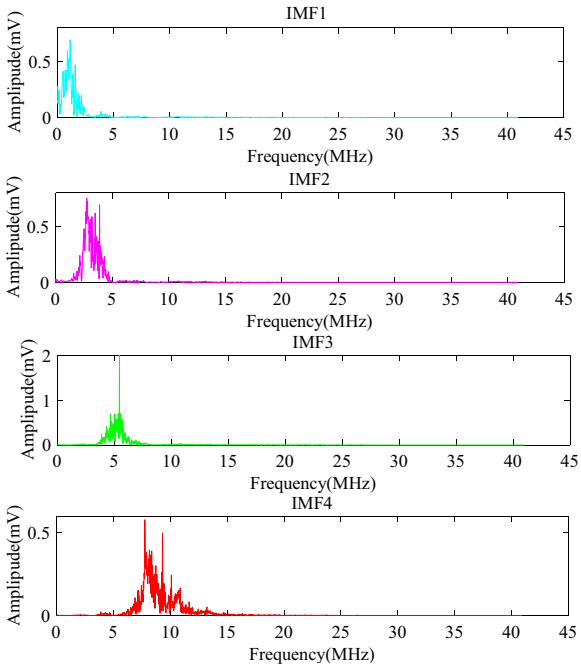

Figure 3 Frequency diagram of the intrinsic modal component when K=4

signal components. Then the corresponding components were reconstructed.

3.2 Enhance Noise Reduction Effect

The WT was used to reduce the noise. The wavelet transform retained local useful information for the signal and removed noise. The phase distortion was guaranteed to affect the echo time accuracy. According to the characteristics of the wavelet basis function and signal to be measured, the appropriate wavelet basis function is selected and the number of decomposition layers N is determined. Therefore, the SymN wavelet was selected, and the maximum value $N = 8$ was taken to ensure its optimal characteristics directly. In addition, the sqtwolog rule was used to adjust the noise level estimation of each layer of the wavelet decomposition. The adaptive threshold value was expressed as shown in Eq. (6):

$$Tr_j = \sigma\sqrt{2\ln(n_j)},\ j = 1,...,J, \tag{6}$$

where Tr_j is the j-level threshold, σ is the standard deviation of noise signal, and n_j is the number of j-level wavelet coefficients.

The hard threshold method could not only preserve the characteristics of the signal but also suppress the white noise. The mathematical expression of the hard threshold function is shown in Eq. (7):

$$\widehat{w}_s(j,k) = \begin{cases} w_s(j,k), |w_s(j,k)| \geq \lambda, \\ 0, |w_s(j,k)| \leq \lambda, \end{cases} \tag{7}$$

where $\widehat{w}_s(j,k)$ is the wavelet estimation coefficient; $w_s(j,k)$ is the wavelet decomposition coefficient, and λ is the threshold.

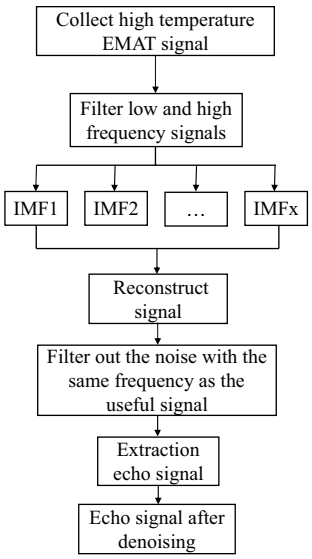

Figure 4 Algorithm flow chart

3.3 Extraction Echo Signal

EEMD-Hilbert was used to extract the echo signal, and the denoised signal was processed with EEMD. The kurtosis factor was used as the index, and the IMF function with the largest kurtosis factor was selected as the final extracted echo signal. The envelope of the ultrasonic signal was extracted with the Hilbert transform. The kurtosis could reflect the signal mutation effectively. The kurtosis value of a signal x_k (k= 1,..., N) could be obtained with Eq. (8):

$$\hat{\gamma}_4 = \frac{E(x_k - \mu)^4}{\sigma^4}, \tag{8}$$

where E is the expected operator, and μ and σ are the mean and standard deviation of the signal.

The Hilbert transform could reflect the instantaneous amplitude and frequency of the signal. The input signal of the Hilbert transform was required to be in a linear steady-state condition. However, in practice, most of the signals were linearly unsteady or even nonlinearly unsteady, and the linear steady-state condition strictly limited the application of the Hilbert transform. The EEMD algorithm could obtain the linear steady signal, and the decomposed IMF had better performance. Therefore, the decomposed signal was used as the input of the Hilbert transform to obtain the envelope.

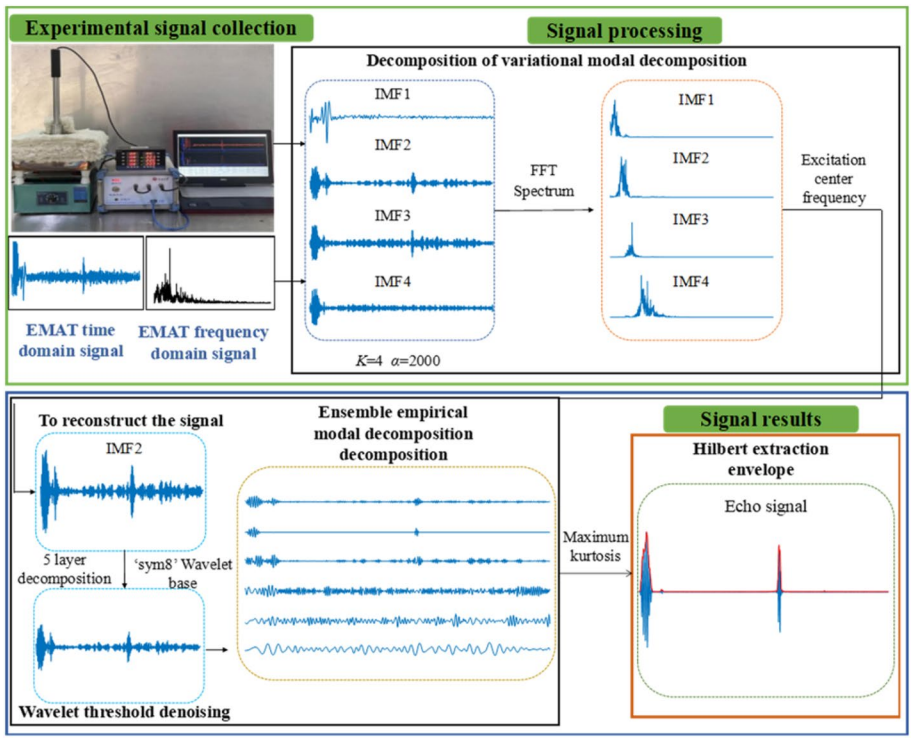

Figure 5 VWEE method diagram

3.4 Algorithm Implementation

The specific algorithm flow of the VWEE method is shown in Figures 4 and 5. The algorithm included the following three steps:

Step 1: The echo signal was decomposed, and the high-frequency and low-frequency noises were filtered. The input signal was decomposed with VMD to obtain the IMFs. The center frequency of the IMF components was calculated with a Fourier transform, which was sequentially arranged from low frequency to high frequency. The appropriate IMF was selected for reconstruction according to the excitation center frequency.

Step 2: The noise with the same frequency in the useful signal was filtered out, improving the effect of noise reduction. The selected IMF components were denoised with the WT, in which the wavelet basis function and the decomposition level were the sym8 wavelet and five-level decomposition, respectively.

Step 3: The echo signal was extracted and the echo information was obtained. After denoising, the signal was processed with EEMD. The kurtosis factor was used as the index, and the IMF function with the largest kurtosis factor was selected as the final extracted echo signal. The envelope of the acoustic signal was extracted with a Hilbert transform.

4 Experiment Setup

The low voltage excitation system is shown in Figure 6. The system was composed of a computer, a self-developed pulsed electromagnetic acoustic detector, a self-developed high-temperature EMAT, a furnace, and the temperature data acquisition equipment.

The computer controlled the EMAT to generate acoustic waves on the surface of the tested sample. The acoustic waves were received by the EMAT and amplified by the amplifier to record in the computer. The test sample was heated by a furnace, which was covered with high-temperature asbestos for thermal isolation. The upper surface of the high-temperature asbestos opened for EMAT placement. Three K-type thermocouples were inserted into the front, middle, and bottom of the test block, crossing the high-temperature asbestos. The three point temperatures were measured to ensure that the samples were heated at a uniform temperature. The EMAT was in direct contact with the front surface of the testing sample. The high-temperature EMAT was self-developed by adding two ceramic thermal insulation layers to the bottom of a normal EMAT [29].

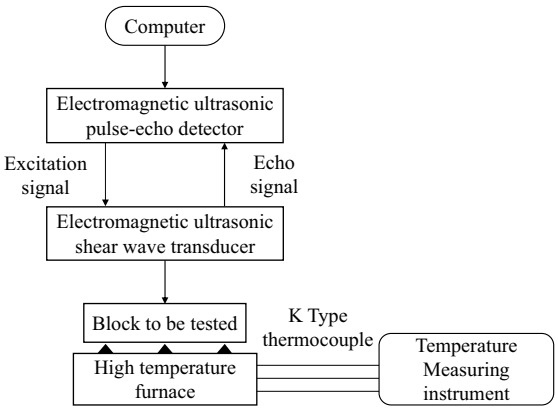

(a) Schematic diagram

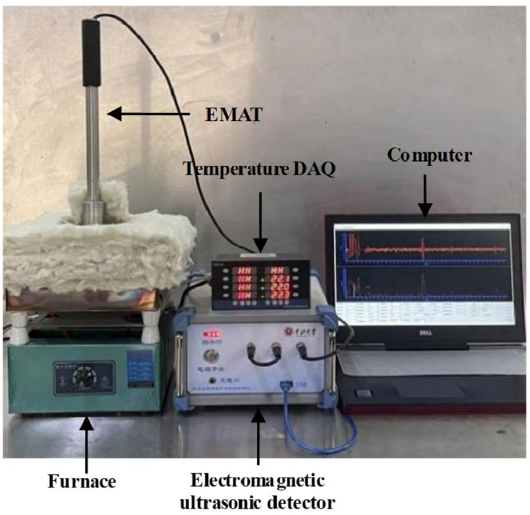

(b) Experiment setup

Figure 6 High-temperature experimental system

In this study, the excitation voltages were 250 V and 35 V for three cycles, and the center frequency was 3.25 MHz. The furnace heated the sample from 25 to 700 °C. The sample were Cr25Mo3Ti, 12CrMo, and Fe.

In the data analysis process, the choice of parameters was critical. In this research, for VMD, to determine the value of the α, a simple test was conducted and it was found that when α was 1500, the noise reduction effect was the best, at 56.5 dB. Because the noise was intense, the Lagrange multiplier was set to zero. The convergence precision ε was 1×10^{-6}. The traditional VMD algorithm required the value of K to be set beforehand, which meant that the signal was decomposed into K modes. After repeated tests, it was found that when K=4, the decomposition effect of the signal was the best. For WT,

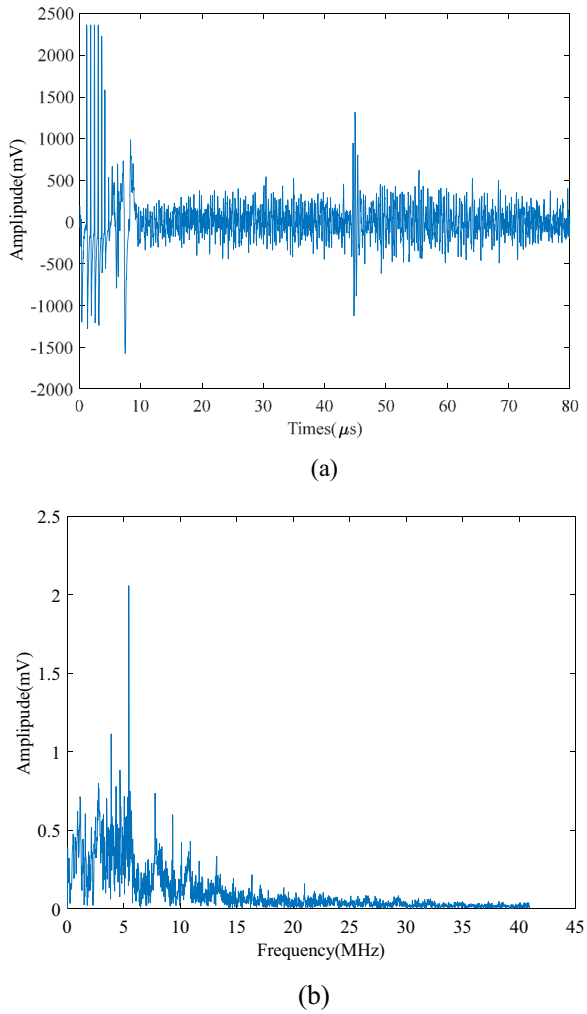

Figure 7 Original ultrasonic signal in (**a**) time domain and (**b**) frequency domain

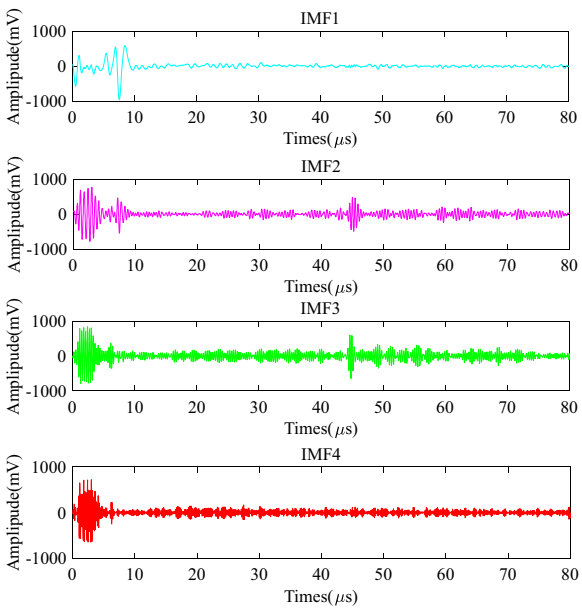

Figure 8 Signal after VMD decomposition in the time domain

the SymN wavelet needed to be selected and the maximum value $N = 8$ was taken to ensure its optimal characteristics directly. The 'sym8' wavelet was selected and the decomposition level was set to 5, which showed the best noise reduction effect with the SNR of 56.1 dB in the test. These choices were based on many repeated experiments. In addition, the sqtwolog rule was used to adjust the noise level estimation of each layer of the wavelet decomposition.

5 Results Analysis and Discussions

5.1 Data Processing

Figure 7 shows the time and frequency domain diagrams of the original signal of 12CrMo at 625 °C. Through acquiring and analyzing data, it was determined that pulsating noise was mainly focused in the low-frequency domain. The resonance phenomenon for EMAT was inevitable, which led to a noise signal and the generation of random fluctuations. This resulted in a deviation of the extreme value point in the envelope extracting process. It was necessary to filter out the noise. Based on the original signal in the time and the frequency domain diagram, the echo signal and some high-frequency electrical noise could be found, as shown in Figure 7(a, b). As the emission signal frequency was presented, the effective echo signal center frequency was distributed around the emission frequency. The high-frequency part was invalid white noise, which did not have any useful information. This caused the SNR of the echo signal to deteriorate, which resulted in the need for filtering.

In the frequency domain, the distribution of the two kinds of noise did not overlap with the effective signal, which provided a signal processing direction. In this research, VMD was used to select the medium and high-frequency IMF where the useful signal resided. This method could effectively filter out the low-frequency noise and the high-frequency noise.

Figures 8 and 3 show the time domain and frequency domain diagrams of the original signals after VMD, respectively. It can be found from Figure 8 that the time domain EMAT signals were successfully decomposed into four IMFs.

Since the pre-set excitation frequency was 3.25 MHz, the useful echo signal was located in IMF 2, which was selected to reconstruct the signal for the VMD, as shown

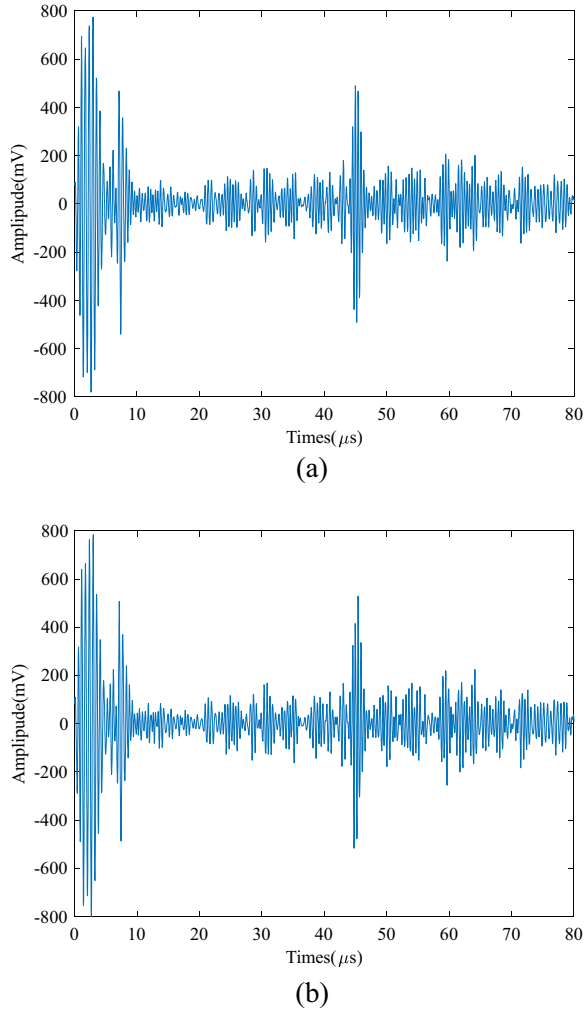

Figure 9 (**a**) Reconstruction signal of VMD decomposition, (**b**) WT denoising signal

in Figure 9(a). Then WT denoising was carried out, as presented in Figure 9(b). The noise reduction method in this research applied to any condition, rather than a fixed excitation frequency. Different excitation frequencies resulted in different center frequencies of ultrasonic echo signals. As an effective time-frequency analysis method, the denoised signal had less interference in narrow-band IMF 2.

To eliminate the noise with a similar frequency to the effective signal, the wavelet denoising method was used. The wavelet can be analyzed in both time and frequency domain and can deal with the abrupt change in the thickness measurement signal. Therefore, before using the signal, it was necessary to conduct further noise reduction processing and improve the SNR.

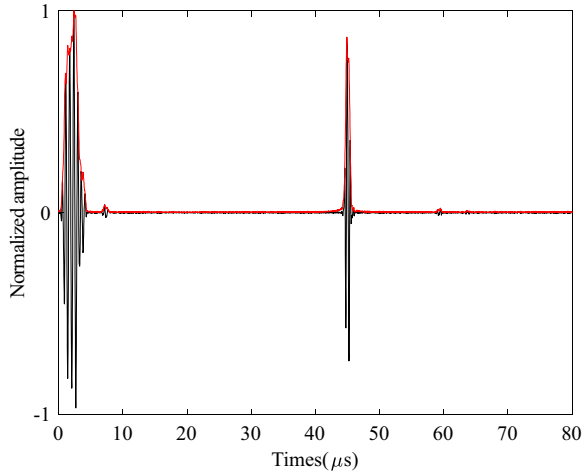

Figure 10 Signal processed with VWEE

The signal noise was effectively suppressed after VMD-WT processing. However, the noise in the signal could not be completely filtered out and the filtering process also suppressed the effective signal. Hence the noise suppression in this link tended to be conservative. Then the EEMD was used for further signal processing. The IMF with the largest kurtosis factor was selected as the final extracted echo signal. Following this, the Hilbert transform was used to extract the envelope of the final signal, as shown in Figure 10. The EEMD method showed an ability to decrease the cumulative errors of the WT and improve the resolution after the time-frequency analysis to eliminate white noise. Furthermore, the Hilbert transform could present the instantaneous amplitude and frequency.

5.2 Comparison of Noise Reduction Ability Among Different Methods

To verify the effectiveness and feasibility of the proposed VWEE method, the same received signal for 12CrMo at 625 °C was selected, with a 250 V excitation voltage, a 50 MHz sampling frequency, and the sampling number of 4096. The following methods were used for noise reduction.

1) VMD: The original signal was decomposed with VMD. The decomposition layer K was set as 4, and the penalty factor α was set as 1500. This method could effectively deal with nonlinear and non-stationary signals. However, it was sensitive to noise. When there was noise, modal aliasing might occur in the decomposition, and the noise suppression ability was weak.

2) WT denoising: The "sym8" wavelet was selected and the decomposition level was set to 5. The hard threshold function was adopted, and the "sqtwolog" rule was used.
3) EMD: The EMD has the disadvantages of mode aliasing and the endpoint effect. The filtering effect could easily produce waveform distortion and it could not retain the original characteristics of the signal to the maximum extent.

To evaluate the advantages and disadvantages of the various methods, the peak SNR was adopted as the evaluation index of the denoising effect. In general, the larger an SNR is, the better the signal denoising effect is.

Equation (9) was used to calculate the SNR, where SNR_{dB} is the SNR of the signal, A_{signal} is the maximum amplitude within a wave packet intercepted, and A_{noise} denotes the average noise amplitude within a selected region next to the echo:

$$SNR_{dB} = 20\lg\frac{A_{signal}}{A_{noise}}. \tag{9}$$

To validate the denoising ability of the method proposed in this paper, several popular denoising methods were compared. Figure 11 gives comparison of the original electromagnetic ultrasonic signal with the signal processed by VMD, WT denoising, and EMD method, respectively. The denoising effect of the other three denoising methods was not ideal, and there were still many noise components in the signal after denoising. As shown in Figure 10, the proposed VWEE denoising method could better preserve the useful part of the signal, and it could effectively remove most of the target signal noise. As adaptive multiresolution techniques, the

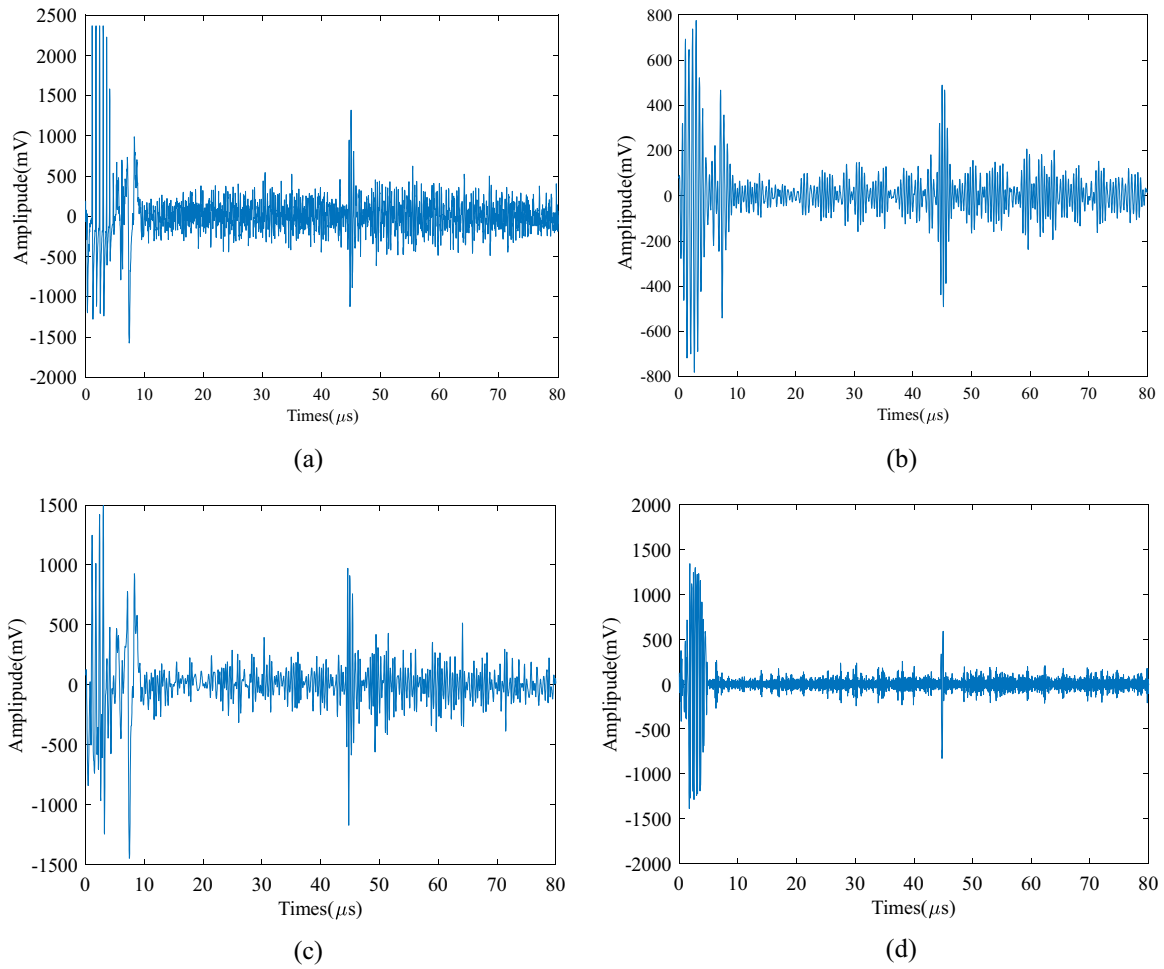

Figure 11 Ultrasonic signal of 12CrMo at 625 °C; (**a**) original signal, (**b**) VMD decomposition and reconstruction signal, (**c**) WT denoising signal, and (**d**) EMD denoising signal

Table 1 Comparison of noise reduction performances of various methods

Denoising method	Original signal	VMD	WT	EMD	VWEE
SNR(dB)	17.6612	18.2363	16.6888	21.3534	55.4574

EMD and VMD could adjust to unknown signal characteristics varying over time. Compared with the VMD, the EMD was more sensitive to noise. The WT-based thresholding technique was better in combination with the VMD method than in use alone.

From Figure 11, the denoising ability of various methods can be seen directly. The SNR values were further compared with the indicator for denoising ability, as shown in Table 1. The higher the SNR of the output signal was, the better the denoised effect was. From Table 1, it can be seen that the denoised effect of VWEE was significantly better than those of the VMD, WT, and EMD methods. The denoising effects of VMD and EMD were similar, and these effects slightly better than those of the WT. Compared with the other methods, the SNR of the high-temperature EMAT signal was improved 2–3 times using the VWEE method.

5.3 Applicability of VWEE Denoising Method for Different Materials at Different Temperatures

To verify the applicability of the denoising method proposed in this study, experiments were conducted on Cr25Mo3Ti and Fe materials. Each specimen of the materials was in the shape of a cake and had a diameter of 100 mm and a thickness of 60 mm. Additionally, all the specimen surfaces were polished. The ultrasonic signal was detected with an excitation voltage of 250 V. All of the samples were heated from 25 to 700 °C. The electromagnetic ultrasonic signals measured at intervals of 50°C were selected for VWEE denoising, and good SNRs were obtained, as shown in Figure 12(a, b). The results demonstrated that the proposed algorithm could be applied to conditions other than a fixed temperature.

As can be seen from Figure 12(a), the SNR of the original electromagnetic ultrasonic signal, detected on the Cr25Mo3Ti specimen from 25 to 700 °C, was the lowest, which was maintained at about 20 dB. Compared with the original signal, the SNR of the signals processed with the WT denoising method and the EMD method was improved to some scale. But the SNR was still low compared with the VWEE method, which was between 50 dB and 60 dB, up to 60.579 dB. The experimental results showed that the VWEE method had a good noise reduction ability for the Cr25Mo3Ti electromagnetic ultrasonic signal, and the echo signal was more obvious, which was more conducive to the extraction of the echo signal information.

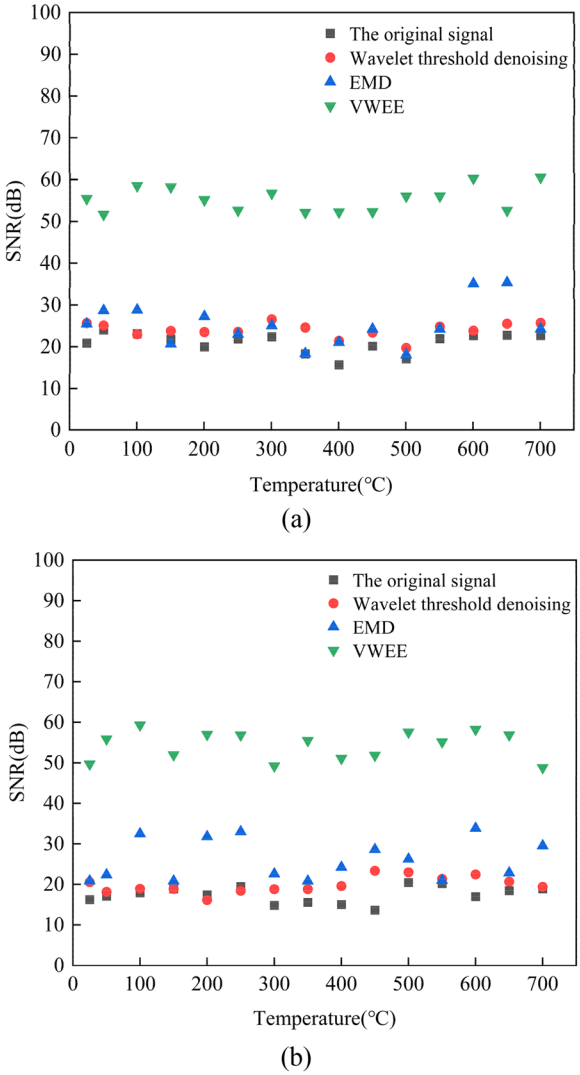

Figure 12 SNR at different temperatures of (**a**) Cr25Mo3Ti and (**b**) Fe

As shown in Figure 12(b), the SNR of the original electromagnetic ultrasonic signal that detected on a Fe specimen from 25 to 700 °C was the lowest, and the signal was maintained between 10 dB and 20 dB. Compared with the original signal, the SNR of the WT denoising method and the EMD method were improved to some extent, but the SNR was still lower than that of the proposed method. The SNR of the electromagnetic ultrasonic signals obtained with the VWEE denoising method was about 50 dB, up to 59.330 dB. The experimental results showed that the VWEE denoising method also had a good denoising effect on Fe, so the proposed method had certain advantages in high-temperature signal processing

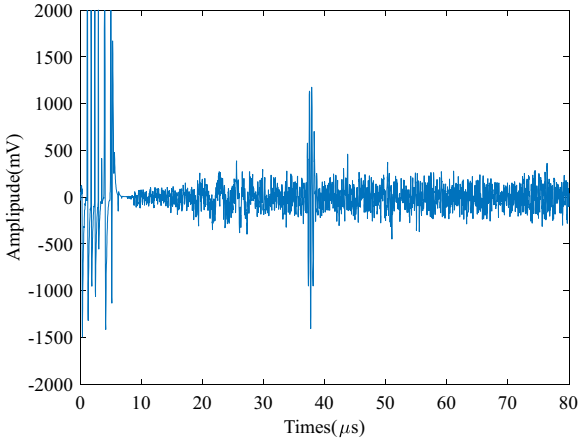

Figure 13 Detection of electromagnetic ultrasonic signals in Cr25Mo3Ti at 25 ℃ and 250 V

compared with the EMD method and the WT denoising method.

5.4 Low Voltage Detection Signal Noise Reduction

Figure 13 shows the original signal of the Cr25Mo3Ti excited at 250 V and 25 ℃. It can be seen from the diagram that the echo signal with 250 V excitation was obvious. As shown in Figure 14, when 35 V low voltage excitation was used, the echo signal was almost buried in the noise signal and the noise level of the system had almost the same amplitude as the effective echoes, so the detection capability could not be provided. The echo signal was obvious after VWEE denoising, which was very important for the actual defect detection of the high-temperature EMAT, both for the detection accuracy and the minimum detection capability. The original electromagnetic ultrasonic signal and the denoising signal for 35 V low voltage detection are shown in Figure 14.

Table 2 shows the SNR of the Cr25Mo3Ti specimen at different temperatures at low excitation voltage before and after VWEE denoising. The SNR of the original signal detected from 25 to 700 °C was about 13 dB, and the echo signal was buried in the noise signal. The SNR after VWEE processing was about 40 dB, with the highest value of 49.878 dB. It can be seen from the table that the proposed method had better noise reduction performance for the Cr25Mo3Ti raw signals at different temperatures. Figure 14 shows the original electromagnetic ultrasonic signal and the VWEE denoising signal of Cr25Mo3Ti for 35 V low-voltage detection from 25 to 700 °C. It can be seen that the original signal was buried in the noise signal and it was difficult to read the echo signal information, which brought some difficulties to detection. The VWEE noise reduction method solved the above problems well, made the echo signal obvious, and preserved the local characteristics of ultrasonic waves.

In this research, the accuracy of the thickness measurement was taken as a new indicator to verify the performance of VWEE. The ultrasonic pulse emitted by the EMAT probe passed through the measured object to the material interface and then reflected to the EMAT probe. The amplitude of the ultrasonic wave gradually decreased. The time difference between the first and second peak of the extracted echo signal could be used to calculate the material thickness, given in Eq. (10):

$$h = v(T) \times \frac{t_2 - t_1}{2}, \tag{10}$$

where $v(T)$ is the shear wave sound velocity of the materials at different temperatures T, h is the thickness of the material, and t_1 and t_2 are the adjacent echo time.

It can be seen from Eq. (10) that the thickness measurement error is mainly affected by the variation of the sound velocity of the material and the time difference between different echo packets. Table 3 shows that the sound velocity of materials changes with the shifting of temperature. In practice, errors caused by the sound velocity changing can be eliminated by calibrating the sound velocity or referring to the standard sound velocity library [30]. However, in electromagnetic ultrasonic detection under high-temperature environment, due to the influence of temperature, the low SNR of the detection signal often leads to the failure in accurately identifying the wave packet. Therefore, the effectiveness of the algorithm can be evaluated by the accuracy of the material thickness calculated by the denoised signal.

The actual thickness of the Cr25Mo3Ti specimen at room temperature was 60 mm. The electromagnetic ultrasonic signals of the Cr25Mo3Ti specimen from 25 to 700 °C were processed with the VWEE noise reduction method in experiments, and the time difference between the first and second echo was calculated to obtain the thickness of the material. The comparison results are presented in Table 3, which shows the effective noise reduction and thickness feature extraction.

6 Conclusions

The VWEE noise reduction method for low SNR electromagnetic acoustic detection was proposed and validated in this research. The following conclusions could be drawn:

(1) Compared with other methods, VWEE had the advantages of the adaptive adjustment of the center frequency of each mode, good noise reduction abil-

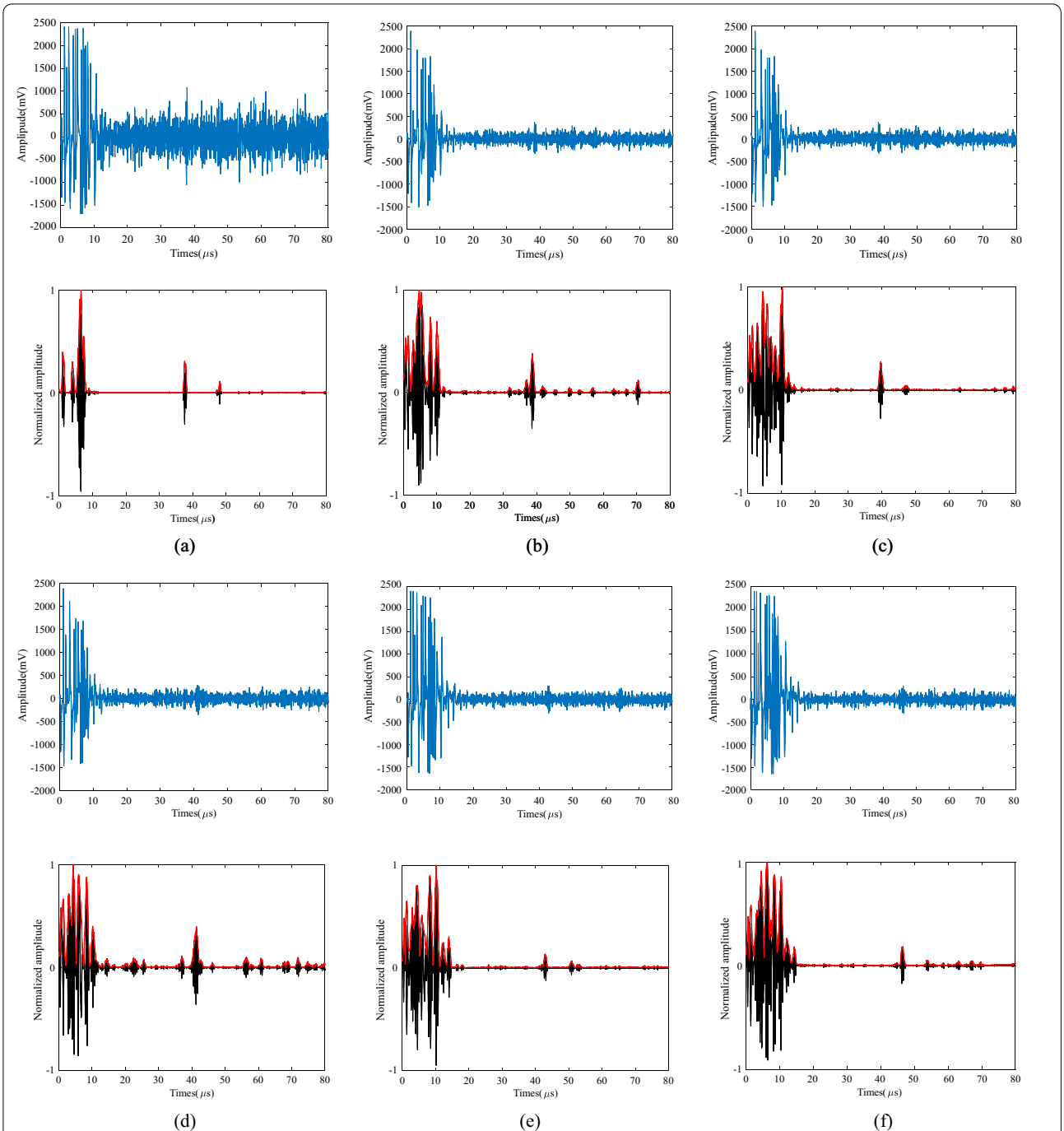

Figure 14 35 V excited original electromagnetic ultrasonic signal and VVWE noise reduction signal at (**a**) 25 °C, (**b**) 150 °C, (**c**) 300 °C, (**d**) 450 °C, (**e**) 550 °C, and (**f**) 700 °C

Table 2 Comparison of the noise reduction performance of Cr25Mo3Ti at different temperatures for low voltage detection

Temperature (℃)	**25**	**150**	**300**	**450**	**550**	**700**
Original signal SNR (dB)	14.8	13.2	14.0	14.5	13.4	13.5
Denoised signal SNR (dB)	49.9	34.6	38.8	43.8	38.3	36.9

Table 3 Thickness measurement of Cr25Mo3Ti at different temperatures

Temperature (℃)	Acoustic Speed [30] (m/s)	Calculated thickness (mm)	Actual thickness (mm)	Error (%)
25	3246	60.25	60	0.4
100	3122	59.57	60.975	2.3
300	3038	59.75	60.994	2.0
500	2870	59.84	61.013	1.8
600	2795	61.62	61.033	0.9
700	2656	61.77	61.062	1.1

ity, and time-frequency analysis of the echo signal, and it could greatly improve the SNR of the EMAT test signal.

(2) Through the experimental analysis of different materials at different temperatures, the VWEE had a good noise reduction effect on the EMAT signals with low SNR when the temperature changed from 25 to 700 °C, making the echo information more obvious.

(3) The VWEE algorithm could extract the echo signal from the strong background noise caused by low-voltage and obtain a smoother envelope and a more accurate peak time. This was significant for ultrasonic detection based on time-of-flight, such as for a thickness gauge or flaw detector.

Acknowledgements
Not applicable.

Author contributions
JZ provided guidance for the whole research, designed the experiment, and wrote the first draft. SZ performed the experiments and analyzed the data. YZ developed the experimental system. XS and JZ put forward suggestions for the manuscript. All authors read and approved the final manuscript.

Authors' Information
Jinjie Zhou, born in 1981, is currently an Associate Professor at *the School of Mechanical Engineering, North University of China, China*. He received his Ph.D. degree from *Beijing University of Technology, China*, in 2012. His research interests include material performance analysis and detection methods in extreme environments, ultrasonic inspecting methods, and instruments.
Shuaijie Zhao, born in 1997, is a master student at *the School of Mechanical Engineering, North University of China, China*. He got his bachelor's degree in 2020. His research interest covers electromagnetic ultrasonic nondestructive testing.
Yang Zheng, born in 1984, is currently a Senior Engineer at *China Special Equipment Inspection and Research Institute, China*. He received his Ph.D. from *Beijing University of Technology, China*, in 2012. His current research interests include new technologies and new equipment for non-destruction testing.
Xingquan Shen, born in 1969, is now a Professor at *the School of Mechanical Engineering, North University of China, China*. He received his Ph.D. degree from the *North University of China, China,* in 2005. His research interests include advanced manufacturing technology and mechanical engineering testing technology.
Jitang Zhang, born in 1963, is now a Professor at *the School of Mechanical Engineering, North University of China, China*. He received his Ph.D. degree from *Beihang University, China,* in 2004. His research interest covers automation detection technology.

Funding
Supported by National Natural Science Foundation of China (Grant No. 62071433) and Shanxi Province Graduate Student Innovation Project (Grant No. 2021Y583).

Competing Interests
The authors declare no competing financial interests.

Author Details
[1]School of Mechanical Engineering, North University of China, Taiyuan 030051, China. [2]China Special Equipment Inspection and Research Institute, Beijing 100029, China.

Received: 12 February 2022 Revised: 27 May 2022 Accepted: 22 July 2022
Published online: 04 September 2022

References

[1] J Brizuela, J Camacho, G Cosarinsky, et al. Improving elevation resolution in phased-array inspections for NDT. *NDT & E International*, 2019, 101(1): 1-16.
[2] S P Song, Y J Ni. Ultrasound imaging of pipeline crack based on composite transducer array. *Chinese Journal of Mechanical Engineering*, 2018, 31: 81.
[3] H Sun, S Huang, Q Wang, et al. Orthogonal optimal design method for point-focusing EMAT considering focal area dimensions. *Sensors and Actuators A-Physical*, 2020, 312: 112109.
[4] J Parra-Raad, P Khalili, F Cegla. Shear waves with orthogonal polarisations for thickness measurement and crack detection using EMATs. *NDT & E international,* 2020, 111: 102212.
[5] J Park, J Lee, J Min, et al. Defects inspection in wires by nonlinear ultrasonic-guided wave generated by electromagnetic Sensors. *Applied Sciences-Basel*, 2020, 10(13): 4479.
[6] G Zhai, B Liang, X Li, et al. High-temperature EMAT with double-coil configuration generates shear and longitudinal wave modes in paramagnetic steel. *NDT & E International*, 2022, 125: 102572.
[7] W Shi, W Chen, C Lu, et al. Interaction of circumferential SH0 guided wave with circumferential cracks in pipelines. *Nondestructive Testing and Evaluation*, 2020, 36(5): 1-26.
[8] M. Hirao, H. Ogi. *Electromagnetic acoustic transducers*. Tokyo: Springer, 2017.
[9] J Tkocz, D Greenshields, S Dixon. High power phased EMAT arrays for nondestructive testing of as-cast steel. *NDT & E International*, 2019, 102: 47-55.
[10] L Yang, I C Ume. Measurement of weld penetration depths in thin structures using transmission coefficients of laser-generated Lamb waves and neural network. *Ultrasonics*, 2017, 78: 96-109.
[11] M Kubinyi, O Kreibich, J Neuzil, et al. Novel S-transform information fusion for filtering ultrasonic pulse-echo signals. *Przeglad Elektrotechniczny*, 2011, 87(1): 290-295.
[12] M Kubinyi, O Kreibich, J Neuzil, et al. EMAT noise suppression using information fusion in stationary wavelet packets. *IEEE Transactions on Ultrasonics Ferroelectrics & Frequency Control*, 2011, 58(5): 1027-1036.
[13] B Lei, P Yi, J Xiang, et al. A SVD-based signal de-noising method with fitting threshold for EMAT. *IEEE Access,* 2021, 9: 21123-21131.
[14] S Legendre, J Goyette, D Massicotte. Ultrasonic NDE of composite material structures using wavelet coefficients. *NDT & E International*, 2001, 34(1): 31-37.
[15] S Huang, Y Tong, W Zhao. A denoising algorithm for an electromagnetic acoustic transducer (EMAT) signal by envelope regulation. *Measurement Science & Technology*, 2010, 21(8): 085206.
[16] N E Huang, Z Shen, S R Long, et al. The empirical mode decomposition and the Hilbert spectrum for nonlinear and non-stationary time series analysis. *Proceedings Mathematical Physical & Engineering Sciences*, 1998, 454(1971): 903-995.

[17] M Sun, S Yi, Z Wei. A wavelet threshold denoising method for ultrasonic signal based on EMD and correlation coefficient analysis. *2010 3rd International Congress on Image and Signal Processing. IEEE: Yantai, China*, 2010: 3992-3996.
[18] Z Wu, N E Huang. Ensemble empirical mode decomposition: A noise-assisted data analysis method. *Advances in Adaptive Data Analysis*, 2009, 1: 1-41.
[19] J M Yu, Z Zhang. Research on Feature Extraction for Ultrasonic Echo Signal Based on EEMD Approach. *Applied Mechanics and Materials*, 2013, 321: 1311-1316.
[20] K Dragomiretskiy, D Zosso. Variational mode decomposition. *IEEE Transactions on Signal Processing*, 2014, 62(3): 531-544.
[21] S Huang, H Sun, S Wang, et al. SSWT and VMD linked mode identification and time-of-flight extraction of denoised SH guided waves. *IEEE Sensors Journal*, 2021, 21(3): 14709-14717.
[22] D Si, B Gao, W Guo, et al. Variational mode decomposition linked wavelet method for EMAT denoise with large lift-off effect. *NDT & E international*, 2019, 107: 102149.
[23] W Wei, L Li, W F Shi, et al. Ultrasonic imaging recognition of coal-rock interface based on the improved variational mode decomposition. *Measurement*, 2020, 170(1): 108728.
[24] F Y Li, B Zhang, S Verma, et al. Seismic signal denoising using thresholded variational mode decomposition. *Exploration Geophysics*, 2018, 49(4): 450-461.
[25] H P Hu, L M Zhang, H C Yan, et al. Denoising and base-line drift removal method of MEMS hydrophone signal based on VMD and wavelet threshold processing. *IEEE Access*, 2019, 7: 59913-59922.
[26] R Ram, M N Mohanty. Performance analysis of adaptive variational mode decomposition approach for speech enhancement. *International Journal of Speech Technology*, 2018, 21(2): 369-381.
[27] X J Gu, C Z Chen. Rolling bearing fault signal extraction based on stochastic resonance-based denoising and VMD. *International Journal of Rotating Machinery*, 2017: 1-12.
[28] W Ren, J He, S Dixon, et al. Enhancement of EMAT's efficiency by using silicon steel laminations back-plate. *Sensors and Actuators A-Physical*, 2018, 274: 189-198.
[29] Y Zheng, Z Li, J J Zhou, et al. Study on the change law of transverse ultrasonic velocity in a high temperature material. *Research in Nondestructive Evaluation*, 2021, 32(1): 38-57.
[30] State Administration for Market Regulation, Standardization Administration of China. GB/T 40730-2021 Non-destructive—Measuring thickness by electromagnetic ultrasonic pulse-echo. Beijing: China Standard Publishing House, 2021. (in Chinese)